Initial Results From the First MEMS Fabricated Thermal Transpiration-Driven Vacuum Pump

Stephen E. Vargo and E. P. Muntz

Dept. of Aerospace and Mechanical Engineering, University of Southern California
854 W. 36th Place, RRB 101, Los Angeles, CA 90089
(213) 740-5312, (213) 740-7774 fax, email: vargo@spock.usc.edu

Abstract. The success of NASA's future space missions and the development of portable, commercial instrument packages will depend greatly on miniaturized components enabled by the use of microelectromechanical systems (MEMS). Both of these application markets for miniaturized instruments are governed by the use of MEMS components that satisfy stringent power, mass, volume, contamination and integration requirements. An attractive MEMS vacuum pump for instruments requiring vacuum conditions is the Knudsen Compressor, which operates based on the rarefied gas dynamics phenomenon of thermal transpiration. Thermal transpiration describes the regime where gas flows can be induced in a system by maintaining temperature differences across porous materials under rarefied conditions. This pumping mechanism provides two overwhelmingly attractive features as a miniature vacuum pump - no moving parts and no working fluids or lubricants. Due to favorable power, volume and mass estimates a Knudsen Compressor fabricated using MEMS fabrication techniques (lithography, deep reactive ion etching) and new materials (silicon, aerogel) has been completed. The experimental testing of this MEMS Knudsen Compressor device's thermal and pumping performance are outlined in this manuscript. Good agreement between experiments and numerical predictions using a transitional flow analysis have also been obtained although simple simulations based on the aerogel's structure are difficult to perform.

INTRODUCTION

Due to recent budgetary concerns the National Aeronautics and Space Administration (NASA) has adopted a smaller, more frequent and focused mission approach for their robotic exploration programs. The success of these missions will undoubtedly rely on the advantages MEMS provide, such as smaller resultant system mass, volume and power consumption values. These benefits have led to governmental as well as commercial interest in the development of portable, integrated analytical instruments. Mass spectrometers, gas chromatographs and on-demand gas generators are some of the devices in various stages of MEMS development. Existing analytical instrument packages at NASA's Jet Propulsion Laboratory (JPL) lack unique and integrated methods towards satisfying their vacuum needs for an array of *in situ* sampling and analyzing missions currently under study. The currently available commercial rough vacuum pumps cannot meet the requirements imposed by the miniaturized analytical instruments proposed for portable use. Commercial pumps are greatly oversized for the small flows needed and pose serious technical challenges towards their miniaturization. In these small instrument systems the vacuum pump tends to have the greatest mass, volume, power consumption and cost penalties. Obviously, miniaturized and possibly integrated vacuum pumps would greatly increase the attractiveness of these types of instruments. The few number of existing miniaturized vacuum pumps, suffer from either negative scaling issues, poor performance, constraining operation or detrimental system impacts. Based on these issues and future NASA mission requirements it is clear that successful MEMS vacuum pumps cannot be simply scaled-down versions of commercially available pumps. The Knudsen Compressor, which was originated at the University of Southern California (USC) in 1993 and is currently in joint development with JPL, is an attractive vacuum pump that can provide pumping of gases in the pressure range of 1 mTorr (possibly down to 0.1 mTorr) to 760 Torr.

Knudsen Compressors have two overwhelmingly attractive features as miniaturized vacuum pumps - no moving parts and no fluids or lubricants. These pumps are driven by the rarefied gas dynamics phenomenon of thermal

CP585, *Rarefied Gas Dynamics: 22nd International Symposium*, edited by T. J. Bartel and M. A. Gallis

transpiration. In many instances thermal transpiration tends to be a laboratory curiosity at normal dimensions and correspondingly low pressures. However, in the micromechanical domain it can form the basis for important systems because free molecular conditions can exist at much higher pressures due to the characteristically smaller dimensions of MEMS structures. The recent availability of nanopore materials with low thermal conductivity and MEMS fabrication techniques have significantly expanded the utilization of thermal transpiration as a pumping mechanism. These developments allow the construction of a thermal transpiration-driven vacuum pump that can operate under free molecular conditions over a wider and more useful pressure range (from about 1 mTorr to above 760 Torr). Through proper materials selection and pump design the Knudsen Compressor aims to utilize this phenomenon in order to create functional MEMS vacuum pumps.

ANALYSIS OF A SINGLE STAGE THERMAL TRANSPIRATION VACUUM PUMP

The single stage analysis presented here is a summary of a detailed analysis presented by Vargo *et al.* [1] for multiple staged Knudsen Compressor operation. Knudsen Compressors generate large changes in pressure for most systems by utilizing a cascade of multiple, individually heated stages. Each stage in the pump consists of a capillary and connector section. A temperature increase across the capillaries results in a thermal transpiration driven pressure increase. The capillary section is followed by a connector section where the pressure is approximately constant while the temperature drops to its original value prior to entering the next stage.

The maximum pressure difference (i.e. no mass flow for steady state conditions) between the hot and cold sides of a single stage Knudsen Compressor is

$$(\Delta p_I)_T = \frac{p_{AVG}\,\Delta T}{T_{AVG}}\left[\frac{Q_T}{Q_P} - \frac{Q_{T,C}}{Q_{P,C}}\right] \tag{1}$$

where p_{AVG}, ΔT and T_{AVG} are the average pressure, temperature difference across the transpiration membrane and the average temperature, respectively. Q_T and Q_P are the thermal transpiration and Poiseuille flow coefficients for cylindrical tubes, respectively. These flow coefficients have been numerically determined and are functions of Kn. The subscript C refers to the connector section of the stage and the flow coefficients without subscript refer to the capillary section. The ratio Q_T/Q_P varies from close to 0.5 near free molecular conditions to $6\text{x}10^{-3}$ near continuum conditions. The operation of the Knudsen Compressor changes dramatically in the transitional flow regime. The average pressure in the stage is identically equal to

$$p_{AVG} = p_0 + \frac{(\Delta p_I)_T}{2} \tag{2}$$

with p_0 the inlet pressure to the stage (i.e. the cold side pressure).

A useful experiment is to measure the change in pressure as a function of time (i.e. throughput) when the Knudsen Compressor pumps gas from one closed volume to another, starting from equal pressures in the two volumes. The instantaneous fractional pressure change is given by

$$\frac{\Delta p_I}{(\Delta p_I)_T} = 1 - e^{(-K_T t)} \tag{3}$$

where the inverse of K_T is the characteristic time needed for Δp_I to reach $(\Delta p_I)_T$. Based on the transitional analysis [1] the constant K_T is found from

$$K_T = \frac{A}{V}\sqrt{\frac{kT_{AVG}}{2m}}\left[\frac{(L_x/L_r)}{FQ_P} + \frac{(L_X/L_R)_C}{Q_{P,C}}\right]^{-1} \tag{4}$$

where A is the cross-sectional area of the capillary membrane, k is Boltzmann's constant, m is the mass of the working gas, F is the fractional open area of the membrane, L_x is the membrane's thickness, L_r is the radius of the membrane pores and $V = (V_C V_H)/(V_C + V_H)$ with V_C and V_H the cold and hot side volumes, respectively.

SINGLE STAGE MEMS KNUDSEN COMPRESSORS

Device Design and Fabrication

The MEMS devices that have been fabricated (see Fig. 1) consist of two silicon chips (thermal guards), which are each 2.025 cm x 2.025 cm and 400 μm thick, an aerogel membrane (520 μm thick), two Corning Pyrex® 7740 plenums and two aluminum vacuum connectors. The silicon chips (a hot side and cold side) and the aerogel, which is a porous membrane made of suspended SiO_2 particles, serve as the improved thermal guards and transpiration membrane in comparison to the proof-of-concept Knudsen Compressors [2,3], respectively. Each silicon chip has been deep reactive ion etched (DRIE) with a dense array of 20 μm diameter holes through the chip's thickness (i.e. cylindrical tubes) for gas passage. A thin gold film heater is also patterned on each silicon chip for the establishment of device temperatures warmer than ambient. The aerogel has an average pore size of 20 nm and a very low thermal conductivity (17 mW/mK at 760 Torr) providing the essential requirements for thermal transpiration to result when a voltage is applied to the heater. In normal operation, the cold side is not actively cooled and remains cooler than the hot side due to the sandwiched aerogel membrane. A thin perimeter bead of Torr Seal® epoxy is used to secure the thermal guards and aerogel together. Pyrex plenums are anodically bonded to the silicon chips and serve as mating pieces to a pair of machined aluminum vacuum connectors. Vacuum tubing is attached to the machined aluminum pieces to connect the device to pumping and gas input lines. Gas pumping in the device is made possible by establishing a temperature gradient across the aerogel membrane using the hot side's heater. The performance of this design using new materials and fabrication techniques is critical to the realization of a Knudsen Compressor cascade composed of many individually operated stages.

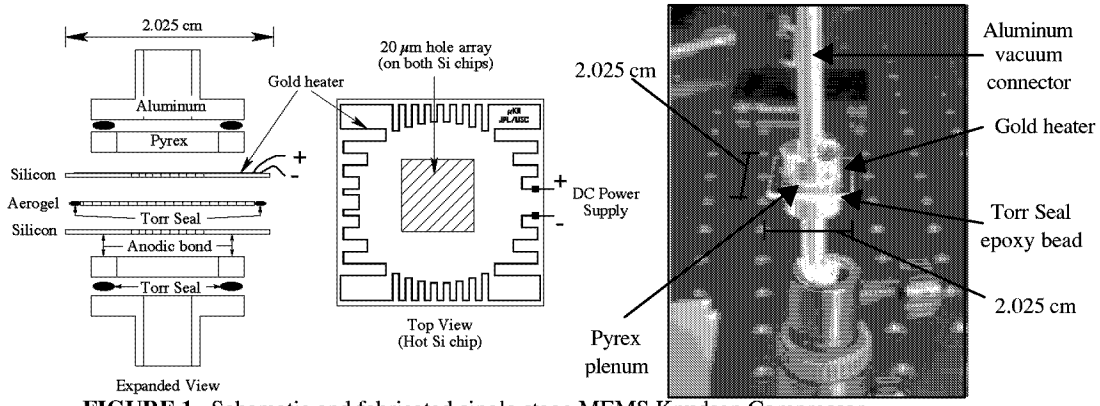

FIGURE 1. Schematic and fabricated single stage MEMS Knudsen Compressor.

MEMS Processing of the Thermal Guards

The DRIE system used for the thermal guard fabrication is an inductively coupled plasma RIE manufactured by Surface Technology Systems (STS) and is available at JPL. Silicon wafers are patterned with photoresist layers in order to selectively etch the desired features. The hole arrays that have been tested consist of 20 μm diameter holes spaced by 40 μm in a central 0.5 cm^2 area per thermal guard (see Fig. 1). The silicon etch process for the thermal guards is outlined in Fig. 2 with the batch fabrication methods of MEMS processing allowing nearly 1.4×10^4 holes to be fabricated simultaneously in each thermal guard (8.75% array open area) with eight thermal guards being fabricated in each 100 mm diameter, 400 μm thick silicon wafer. A front and back side etch using the STS DRIE creates the 20 μm diameter hole array in the silicon wafers. Back side alignment using wafer and mask alignment

marks allows the front and back side features to align within ± 1 μm (see Fig. 3). The jagged features shown in this scanning electron micrograph of a test sample hole array are partial silicon tubes that remained after cleaving.

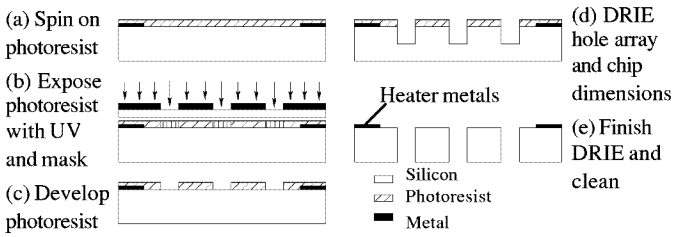

Figure 2. Processing steps for the DRIE of the thermal guards.

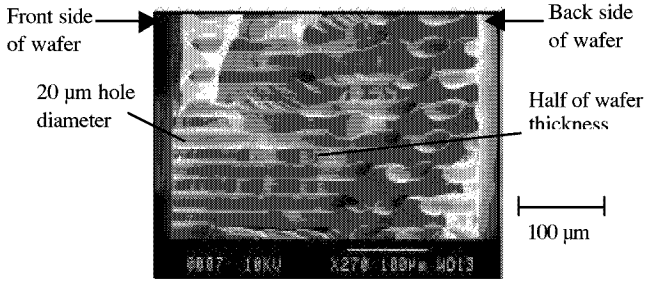

Figure 3. Alignment check for the etched thermal guard hole array.

Aerogel as a Thermal Transpiration Membrane

Thermal transpiration over useful pressure ranges in a Knudsen Compressor requires the use of a material that has both low thermal conductivity and small internal pores. The use of an aerogel membrane enables the construction of a MEMS version of the Knudsen Compressor. Aerogels are a special class of continuously porous solid materials characterized by nanometer size particles and pores. It's rather empty structure (see Fig. 4) results in a thermal conductivity that varies with the ambient pressure (17 mW/mK at 760 Torr and 8 mW/mK at $p<1$ Torr) [4]. Particles of diameters 2-5 nm and pores of diameters 10-100 nm, produce a solid-gas matrix in which the volume fraction of the solid can be less than 5%. The pore size distribution for aerogels, which make direct numerical simulations difficult, can be obtained by N_2 adsorption/condensation analysis [5]. In the MEMS Knudsen Compressor a plain silica based aerogel has been used and its thickness and mean pore size are 520 μm and 20 nm (this gives $Kn = 6.4$ for air at 760 Torr), respectively.

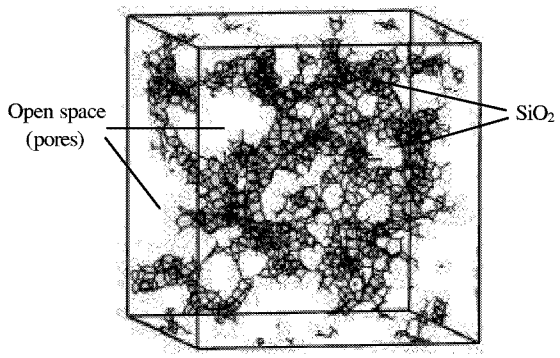

Figure 4. Schematic description of aerogel's structure [5].

Vacuum tight sealing of the various Knudsen Compressor components is imperative to determining device performance under experimental conditions. The small pressures differences generated (< 20 Torr) across a single stage dictate that the experimental device and system be leak tight. Even small leaks are intolerable since they cannot be distinguished from the thermal transpiration pressure increases. Anodic bonding of the Pyrex plenums to the silicon thermal guards ensures the required vacuum seal. A thin bead of Torr Seal epoxy around the perimeter of the thermal guard and aerogel membrane sandwich was found to be the best method of forming this seal. An additional epoxy bond between each Pyrex and aluminum piece provide the remaining vacuum seals.

The epoxy bond between the thermal guards and the aerogel membrane is the bond of interest in the MEMS devices. Two identically fabricated single stage devices, which are referred to as μKn1 (first version) and μKn2 (second version), were epoxy bonded near the aerogel slightly different in order to investigate the impact this epoxy would have on device performance (see Fig. 5). The first version was assembled using two separate beads of epoxy to validate the epoxy as a viable sealing approach and to ensure that the device was leak tight. The second device used a wider aerogel membrane that was the same dimensions as the thermal guard chips and only had one epoxy bead around the perimeter of the device thickness. This is done in order to minimize the heat conduction path between the hot and cold thermal guards since Torr Seal has a much higher thermal conductivity than aerogel (about 26 times greater). These bonding approaches result in different device heat transfer, which correspond to different performance, due to the location and amount of epoxy used. Less heat transfer for the same input heater power was seen for μKn2 in comparison to μKn1.

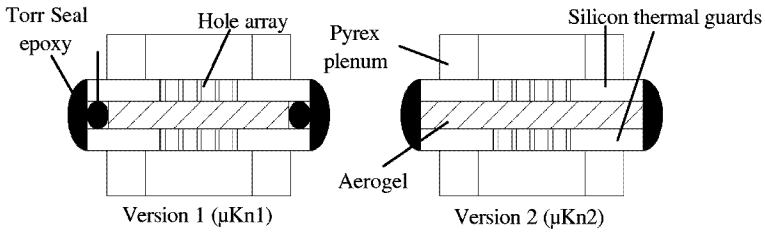

Figure 5. Different epoxy bond approaches for the two single stage devices.

RESULTS AND DISCUSSION

Experimental Layout

The experimental setup for the single stage MEMS Knudsen Compressor devices is shown in Fig. 6. Each device is connected to the rest of the vacuum system using lengths of plastic and stainless steel tubing. The tubing is connected to each other and to other components using an assortment of Swagelok® vacuum fittings. This system is pumped out to low pressures using a mechanical pump that provides an ultimate pressure of about 230 mTorr when either MEMS device is included in the system. Working gases, which were Ar, CO_2, He and N_2, from regulated, high-pressure gas bottles are introduced into the system. The thermal transpiration efficiency will depend on the actual working gas. Helium remains more rarefied than does CO_2 at the same pressure and hence leads to better performance. Absolute pressures in the system are measured using a 10 Torr and 1000 Torr MKS Instruments Baratron® absolute pressure transducers (type 122). Pressure differences between the output (hot side) and input (cold side) of the devices are measured using a 10 Torr Baratron® differential pressure transducer (type 223). Temperatures on the silicon thermal guards are found using small, accurately placed thermocouples. Power is supplied to each MEMS device's heater using a DC power supply (0-60 V, 0-1 A), BNC cables and a pair of micropositioner probes. Each probe allows the accurate placement of a thin (12 μm diameter) tungsten tip to one end of the heater. These probes provide electrical contact between the power supply output and input BNC cables and the thin-film heater. Two digital Fluke 87 III multimeters are also connected in the system in order to measure the voltage drop across the heater and the current through the heater (see Fig. 6). In order to investigate the

usefulness of the fabricated MEMS single stage devices and their corresponding maximum pressure differentials $\left((\Delta p_1)_T\right)$ and throughput experiments were conducted.

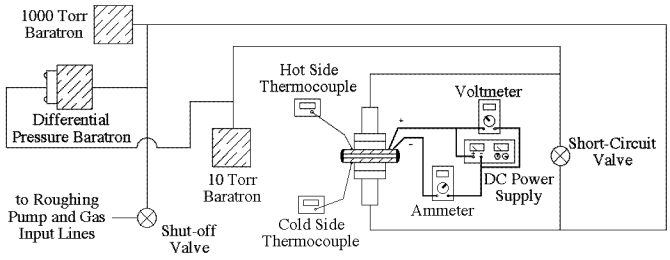

Figure 6. Experimental layout of the MEMS single stage devices.

Constant System Pressure Experiments

Maximum pressure differential measurements $\left((\Delta p_1)_T\right)$ at varying heater temperatures have been made for both MEMS single stage devices under a constant system pressure of 760 Torr using Ar, CO_2, He and N_2 working gases. These $(\Delta p_1)_T$ values, which are measured using the differential Baratron, are made by closing the short-circuit valve (see Fig. 6) and noting the maximum attainable pressure difference between the two sides of the devices. The short-circuit valve is closed only when an established temperature has been reached for any given heater power input. In order to investigate the performance of each device for a given working gas the input power to the heaters was increased by increasing the voltage from the DC power supply. Increases in the voltage drop across the heater result in increased hot side temperatures. Higher temperatures generally result in larger $(\Delta p_1)_T$ values at the same pressure. Figure 7a shows the results for both single stage devices when operated on He and N_2. Note that the $(\Delta p_1)_T$ values have been normalized by the inlet system pressure (p_0), which is the pressure measured on the cold side of the device, in order to properly compare the results from each device.

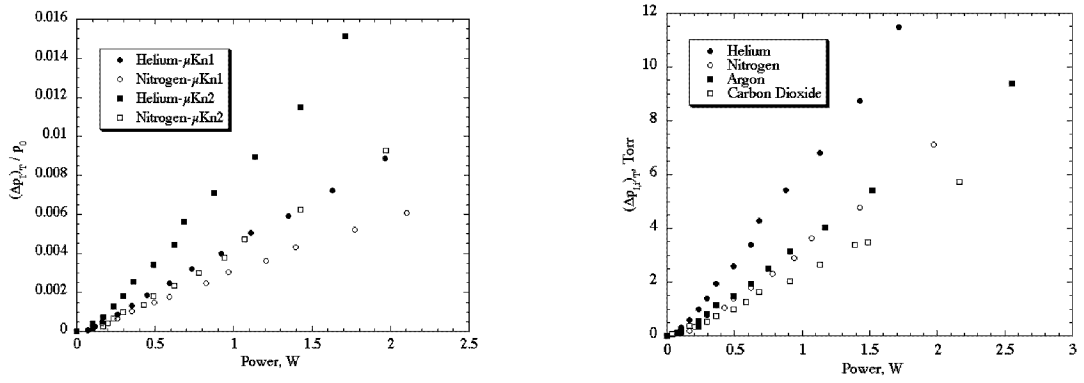

(a) **(b)**

Figure 7a). Differential pressure results for both MEMS devices for 760 Torr operation on He and N_2 with varying heater power. **b).** Differential pressures obtained with μKn2 at 760 Torr operation and various working gases.

As expected, He has a much better performance for the same input power in each device. It is interesting to note that the μKn2 device has significantly better performance than the μKn1 device. At a device input power of 1.5 W, the $(\Delta p_1)_T$ values at p_0 = 760 Torr for the He μKn1, He μKn2, N_2 μKn1 and N_2 μKn2 cases are 5.08 Torr, 9.54 Torr, 3.39 Torr and 5.09 Torr, respectively. The He μKn2 data is 1.88 times higher than the He μKn1 data and the N_2 μKn2 data is 1.5 times higher than the N_2 μKn1 data at this heater power. These factors become larger as the

heater power is increased. These differences between the two devices can be attributed to their slightly different epoxy sealing approaches (see Fig. 5). Since the second MEMS device (μKn2) appears to function better for the same operational inputs it is important to discuss the impact working gas has on device performance. The $(\Delta p_1)_T$ values for Ar, CO_2, He and N_2 for the μKn2 device are included in Fig. 7b. At a heater input power of about 1.7 W the resultant $(\Delta p_1)_T$ for He and CO_2 are about 11.5 Torr and 4.3 Torr, respectively. This is roughly a factor of 2.7 times better when operating on He instead of CO_2.

Constant Heater Power Experiments

In order to investigate the effect varying the Kn has for the same gas and temperature gradient the power (i.e. voltage) to the heater was kept constant. Each device was set to a constant voltage, which maintained a consistent and steady thermal gradient across each device, and then the pressure was varied in order to study the Kn effect. The μKn2 device was set to 14.5 V and this corresponded to a measured ΔT of 2 K at an average temperature of about 304 K and a heater input power of 0.875 W. Figure 8 outlines the μKn2 device results when varying the inlet pressure under constant heater power conditions. It is interesting to restate that μKn2 has greater overall $(\Delta p_1)_T$ values than does μKn1 but both lose efficiency as the inlet pressure approaches atmospheric pressure. Helium remains linear for the entire pressure range but the other gases result in a performance loss at the higher pressures.

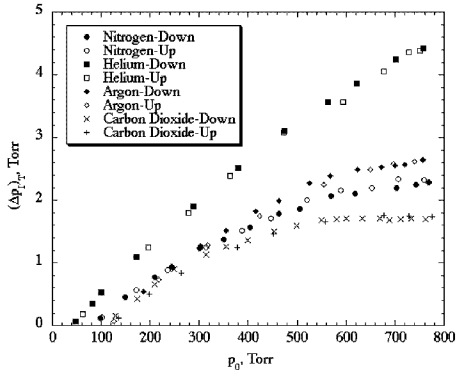

Figure 8. Constant heater power results for μKn2 and varying inlet pressure.

Throughput Experiments

The throughput has been obtained for both single stage devices at a system pressure of about 760 Torr. These measurements are determined by noting the pressure increase in the differential pressure transducers as a function of time. The measurement run is completed when the $(\Delta p_1)_T$ value is reached. Each run corresponded to a constant heater power input to ensure that the temperature remained steady during the measurements. The μKn2 device was tested using 17.5 V (1.15 W) and 20.5 V (1.89 W). Representative throughput curves for the μKn2 lower voltage case are shown in Fig. 9a. It was found that the μKn2 device pumps gas faster than does the μKn1 device. The μKn2 device reached $(\Delta p_1)_T$ values in roughly 100 s but the μKn1 device required an average of 200 s. Note that the N_2 curves are the slowest due to slower thermal speed of N_2 molecules in comparison to He.

Throughput estimates of the single stage devices can be made using Eqns. (3) and (4) with the experimental conditions. Since the aerogel's pore structure is not a collection of cylindrical tubes (see Fig. 4) an uncertainty exists in the effective pore size and thickness of the membrane that should be used in these equations. Due to the maximum pressure differential results presented earlier the average pore size is most likely the same as the quoted value of approximately 20 nm. However, the effective thickness that these pores maintain in the bulk of the material is uncertain. In order to investigate this, several L_x values have been used to generate throughput estimates for the μKn2 device's He curve at 17.5 V. These curves using the measured L_x (520 μm) and several other thickness values with the experimental data are shown in Fig. 9b. Note that the L_x = 52 μm case provides reasonable agreement with the experimental data implying that there are areas of constant sized pores present in the membrane.

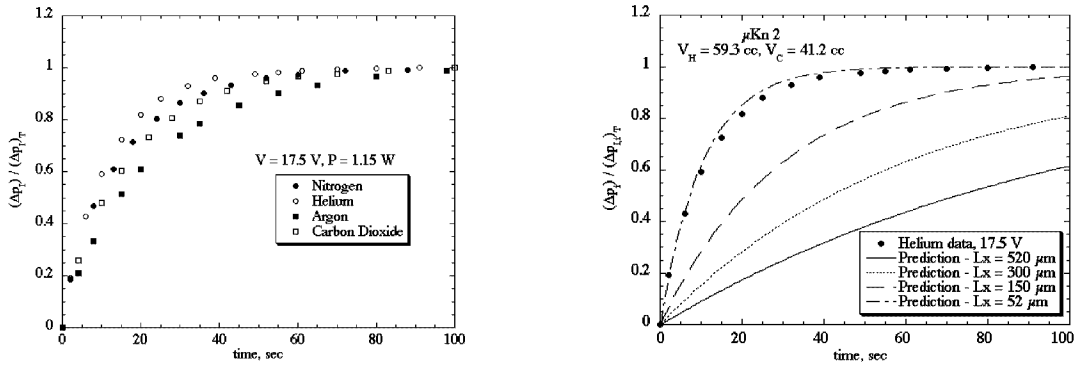

(a) **(b)**

Figure 9a). Throughput curves for μKn2 using a 17.5 V heater voltage. **b).** Throughput curves for the determination of the aerogel's effective membrane thickness.

CONCLUSIONS

Future missions and portable applications that utilize vacuum pumped instruments will most likely require novel and integrated MEMS based vacuum pumps. Many conventional vacuum pumps are incapable of being simply scaled down and are not able to meet the demanding mass, volume power and performance requirements of instrument designers. The MEMS Knudsen Compressor is an attractive roughing pump for these types of applications since it has no moving parts and no dependence on fluids or lubricants. From the results presented in the previous section it is clear that the new materials and fabrication methods have resulted in a functional MEMS single stage Knudsen Compressor. The $(\Delta p_I)_T$ and throughput for each device have shown that device assembly is a critical component of building thermal transpiration devices at the microscale. Example calculations for this vacuum pump resulted in a pump of low energy use, small volume and mass. The successful experimental testing of the single stage MEMS devices has provided insight and feasibility for the design and construction of microscale vacuum pumps based on thermal transpiration.

ACKNOWLEDGMENTS

The research described in the paper was performed jointly by the Center for Space Microelectronics Technology, Jet Propulsion Laboratory, California Institute of Technology and the University of Southern California. It was sponsored by NASA's Office of Space Science and USC.

REFERENCES

1. Vargo, S. E., Muntz, E. P., Shiflett, G. R., and Tang, W. C., *J. Vacuum Science and Technology A* **17**, 2308-2313 (1999).
2. Vargo, S. E., and Muntz, E. P., "A Simple Micromechanical Compressor and Vacuum Pump for Flow Control and Other Distributed Applications," *American Institute of Aeronautics and Astronautics, 34th Aerospace Sciences Conf.*, AIAA-96-0310, Reno, NV, 1996.
3. Vargo, S. E., and Muntz, E. P., "An Evaluation of a Multiple-Stage Micromechanical Knudsen Compressor and Vacuum Pump," in *20th International Symposium on Rarefied Gas Dynamics*, edited by C. Shen, Peking University Press, Beijing, China, 1996, 995-1000.
4. Silica Aerogels - Thermal Properties, website http://eande.lbl.gov/ECS/Aerogels/satcond.htm/, last updated May 5, 1999.
5. Hua, D. W., Anderson, J., Di Gregorio, J., Smith, D. M., and Beaucage, G., *J. Non-Crystalline Solids* **186**, 142-148 (1995).